

Factors determining nestedness in complex networks

Samuel Jonhson¹, Virginia Domínguez-García², Miguel A. Muñoz^{2,*}

¹ Department of Mathematics, Imperial College London, SW7 2AZ, United Kingdom.

² Departamento de Electromagnetismo y Física de la Materia e Instituto Carlos I de Física Teórica y Computacional. Universidad de Granada, E-18071 Granada, Spain. * E-mail: mamunoz@onsager.ugr.es

Abstract

Understanding the causes and effects of network structural features is a key task in deciphering complex systems. In this context, the property of *network nestedness* has aroused a fair amount of interest as regards ecological networks. Indeed, Bastolla *et al.* introduced a simple measure of network nestedness which opened the door to analytical understanding, allowing them to conclude that biodiversity is strongly enhanced in highly nested mutualistic networks. Here, we suggest a slightly refined version of such a measure and go on to study how it is influenced by the most basic structural properties of networks, such as degree distribution and degree-degree correlations (i.e. assortativity). We find that heterogeneity in the degree has a very strong influence on nestedness. Once such an influence has been discounted, we find that nestedness is strongly correlated with disassortativity and hence –as random (neutral) networks have been recently found to be naturally disassortative– they tend to be naturally nested just as the result of chance.

Introduction

Networks have become a paradigm for understanding systems of interacting objects, providing us with a unifying framework for the study of diverse phenomena and fields, from molecular biology to social sciences [1]. Most real networks are not assembled randomly but present a number of non-trivial structural traits such as the small-world property, scale freeness, hierarchical organization, etc [2,3]. Network topological features are essential to determine properties of complex systems such as their robustness, resilience to attacks, dynamical behavior, spreading of information, etc. [3–5]. A paradigmatic case is that of ecosystems, in which species can be visualized as nodes of a network and their mutual interactions (predation, mutualism, etc) encoded in the edges or links. In this context, the solution to May’s famous paradox [6] –the fact that large ecosystems seem to be especially stable, while random matrix theory predicts the contrary– is still not fully clear, but it is widely suspected that there are structural (non random) features of ecological networks at the basis of enhanced stability, which as yet elude us (see [7] for a recent challenge to this idea).

One such feature of ecological networks, which has been studied for some time by ecologists, is called *nestedness* [8]. Loosely speaking, a bipartite network [3] –say, for argument’s sake, of species and islands, linked whenever the former inhabits the latter– is said to be nested if the species that exist on a few islands tend always to be found also on those islands inhabited by many different species. This can be most easily seen by graphically representing a matrix such

that species are columns and islands are rows, with elements equal to one whenever two nodes are linked and zero if not. If, after ordering all nodes by degree (number of neighbours), most of them can be quite neatly packed into one corner, the network is considered highly nested [8,9]. This is illustrated in Fig.1 where we plot different connectivity matrices with different levels of maximal “compactability” and, thus, with different levels of nestedness.

Nestedness is usually measured with purposely-designed software. The most popular *nestedness calculator* is the “temperature” of Atmar and Patterson (used to extract a temperature from the matrices in Fig.1) [8]. It estimates a curve of equal density of ones and zeros, calculates how many ones and zeros are on the “wrong” side and by how much, and returns a number between 0 and 100 called “temperature” by analogy with some system such as a subliming solid. A low temperature indicates high nestedness. It is important to caution that nestedness indices should not be used as black-boxes, as this can lead to false conclusions [10,11]. The main drawback of these calculators is that they are defined by complicated algorithms, hindering further analytical developments. Even if initially introduced for bipartite networks, the concept of nestedness can be readily generalized for generic networks.

In a seminal work, Bascompte and collaborators [12] showed that real *mutualistic networks* (i.e. bipartite networks of symbiotic interactions), such as the bipartite network of plants and the insects that pollinate them, are significantly nested. They also defined a measure to quantify the average number of shared partners in these mutualistic networks, and called it “nestedness” because of its close relation with the concept described above. They go on to show evidence of how the so-defined nestedness of empirical mutualistic networks is correlated with the biodiversity of the corresponding ecosystems [13]: the global species competition is significantly reduced by developing a nested network architecture and this entails a larger biodiversity. The principle behind this is simple. Say nodes A and B are in competition with each other. An increase in A will be to B’s detriment and vice-versa; but if both A and B engage in a symbiotic relationship with node C, then A’s thriving will stimulate C, which in turn will be helpful to B. Thus, the effective competition between A and B is reduced, and the whole system becomes more stable and capable of sustaining more nodes and more individuals. The beneficial effect that “competing” nodes (i.e. those in the same side of a bipartite network) can gain from sharing “friendly” partners (nodes in the other side) is not confined to ecosystems. It is expected also to play a role, for instance, in financial networks or other economic systems [14]. To what extent the measure introduced by Bascompte et al. is related to the traditional concept of nestedness has not, to the best of our knowledge, been rigorously explored. Irrespectively of this relation, however, the insight that mutual neighbours can reduce effective competition in a variety of settings is clearly interesting in its own right, and it is for this reason that we analyse this feature here. On a different front, Staniczenko et al. [15] have made some promising analytical progress regarding the traditional concept of nestedness.

Here, we take up this idea of shared neighbours (though characterized, owing to reasons we shall explain in the Methods, with a slightly different measure) and study analytically and computationally how it is influenced by the most relevant topological properties, such as the degree distribution and degree-degree correlations. Our aim is to understand to what extent nestedness is a property inherited from imposing a given degree distribution or a certain type of degree-degree correlations.

Methods: Analytical quantification of nestedness

Consider an arbitrary network with N nodes defined by the adjacency matrix \hat{a} : the element \hat{a}_{ij} is equal to the number of links (or edges) from node j to node i (typically considered to be either 1 or 0 though extensions to weighted networks have also been considered in the literature [15]). If \hat{a} is symmetric, then the network is undirected and each node i can be characterized by a degree $k_i = \sum_j \hat{a}_{ij}$.¹

Bastolla *et al.* [13] have shown that the effective competition between two species can be reduced if they have common neighbours with which they are in symbiosis. Therefore, in mutualistic networks it is beneficial for the species at two nodes i and j if the number of shared symbiotic partners, $\hat{n}_{ij} = \sum_l \hat{a}_{il} \hat{a}_{lj} = (\hat{a}^2)_{ij}$, is as large as possible. Going on this, and assuming the network is undirected, the authors propose to use the following measure:

$$\eta_B = \frac{\sum_{i < j} \hat{n}_{ij}}{\sum_{i < j} \min(k_i, k_j)}, \quad (1)$$

which they call *nestedness* because it would seem to be highly correlated with the measures returned by nestedness software. Note that, although the authors consider only bipartite graphs, such a feature is not imposed in the above definition.

Here, we take up the idea of the importance of having an analytical expression for the nestedness but, for several reasons, we use a definition slightly different from the one in [13]. Actually, η_B suffers from a serious shortcoming; if one commutes the sums in the numerator of Eq.(1), it is found that the result only depends on the heterogeneity of the degree distribution: $\sum_{i < j} \hat{n}_{ij} = \sum_l \sum_i \hat{a}_{il} \sum_j \hat{a}_{lj} = N \langle k^2 \rangle$.² Therefore, this index essentially provides a measurement of network heterogeneity. Also, although the maximum value \hat{n}_{ij} can take is $\min(k_i, k_j)$, this is not necessarily the best normalization factor, since (as we show explicitly in the next Section) the randomly expected number of paths of length 2 connecting nodes i and j depends on both k_i and k_j . Furthermore, it can sometimes be convenient to have a local measure of nestedness (i.e. nestedness of any given node) which cannot be inferred from the expression above. For all these reasons, we propose to use

$$\tilde{\eta}_{ij} \equiv \frac{\hat{n}_{ij}}{k_i k_j} = \frac{(\hat{a}^2)_{ij}}{k_i k_j}, \quad (2)$$

which is defined for every pair of nodes (i, j) . This allows for the consideration of a nestedness per node, $\tilde{\eta}_i = N^{-1} \sum_j \tilde{\eta}_{ij}$, or of the global measure

$$\tilde{\eta} = \frac{1}{N^2} \sum_{ij} \tilde{\eta}_{ij} \quad (3)$$

which is very similar in spirit to the measure introduced by Bastolla *et al.* in [13] but, as argued above, has a number of additional advantages. This new index can be easily applied to bipartite networks, as shown in Appendix A.

¹If it is directed, i has both an *in* degree, $k_i^{\text{in}} = \sum_j \hat{a}_{ij}$, and an *out* degree, $k_i^{\text{out}} = \sum_j \hat{a}_{ji}$; we shall focus here on undirected networks, although most of the results could be easily extended to directed ones.

²In an undirected network, $\sum_{i < j} = \frac{1}{2} \sum_{ij}$; we shall always sum over all i and j , since it is easier to generalize to directed networks and often avoids writing factors 2.

Having an analytical definition of nestedness, it becomes feasible to scrutinize how it is influenced by the most basic structural features, such as the degree distribution and degree-degree correlations. The standard procedure to determine how significantly nested a given network is, is to generate randomizations of it (while keeping fixed some properties such as the total number of nodes, links, or degree distribution) and compare the nestedness of the initial network with the ensemble-averaged one. The set of features kept fixed in randomizations determine the *null-model* used as reference.

Effects of the degree distribution: configuration model

Many networks have quite broad degree distributions $P(k)$; most notably the fairly ubiquitous scale-free networks, $P(k) \sim k^{-\gamma}$ [2]. Since heterogeneity tends to have an important influence on any network measure, it is important to analytically quantify the influence of degree-distributions on nestedness. For any particular degree sequence, the most natural choice is to use the *configuration model* [3, 16] –defined as the ensemble of random networks wired according to the constraints that a given degree sequence (k_1, \dots, k_N) is respected– as a *null model*. In such an ensemble, the averaged value of any element of the adjacency matrix is

$$\overline{\hat{a}_{ij}} \equiv \epsilon_{ij}^c = \frac{k_i k_j}{\langle k \rangle N}. \quad (4)$$

We use an overline, $\overline{(\cdot)}$, to represent ensemble averages and angles, $\langle \cdot \rangle$, for averages over nodes of a given network.

Nestedness in the configuration model

Plugging Eq. (4) into Eq. (2), we obtain the expected value of $\tilde{\eta}$ in the configuration ensemble, which is our basic null model

$$\overline{\tilde{\eta}_{ij}} = \frac{\langle k^2 \rangle}{\langle k \rangle^2 N} \equiv \tilde{\eta}_{conf}. \quad (5)$$

It is important to underline that $\overline{\tilde{\eta}_{i,j}}$ is independent of i and j ; hence, it coincides with the expected value for the global measure, $\overline{\tilde{\eta}} = \overline{\tilde{\eta}_{i,j}}$ (which justifies the normalization chosen in Eq. (2)). Also, it is noteworthy that for degree distributions with finite first and second moments, $\tilde{\eta}_{conf}$ goes to zero as the large-N limit is approached.

It is obvious from Eq. (5) that degree heterogeneity has an important effect on $\tilde{\eta}$; for instance, scale-free networks (with a large degree variance) are much more nested than homogeneous ones. Therefore, if we are to capture aspects of network structure other than those directly induced by the degree distribution it will be useful to consider the nestedness index normalized to this expected value,

$$\eta \equiv \frac{\tilde{\eta}}{\tilde{\eta}_{conf}} = \frac{\langle k \rangle^2}{\langle k^2 \rangle N} \sum_{ij} \frac{(\hat{a}^2)_{ij}}{k_i k_j}. \quad (6)$$

Although η is unbounded, it has the advantage that it is equal to unity for any uncorrelated random network, independently of its degree heterogeneity, thereby making it possible to detect additional non-trivial structure in a given empirical network.

Degree-degree correlations in the configuration model

In the configuration ensemble, the expected value of the mean degree of the nearest neighbours (nn) of a given node is $\overline{k_{nn,i}} = k_i^{-1} \sum_j \hat{e}_{ij}^c k_j = \langle k^2 \rangle / \langle k \rangle$, which is independent of k_i . Still, specific finite-size networks constructed with the configuration model can deviate from the ensemble average results (which hold exactly only in the $N \rightarrow \infty$ limit). Real networks are finite, and they often display degree-degree correlations, which result in $\overline{k_{nn,i}} = \overline{k_{nn}}(k_i)$. If $\overline{k_{nn}}(k)$ increases (decreases) with k , the network is said to be assortative (disassortative), i.e. nodes with large degree tend to be connected with other nodes of large (small) degree.

The measure usually employed of this phenomenon is Pearson's coefficient applied to the edges [3, 4, 17]: $r = ([k_l k'_l] - [k_l]^2) / ([k_l'^2] - [k_l]^2)$, where k_l and k'_l are the degrees of each of the two nodes belonging to edge l , and $[\cdot] \equiv (\langle k \rangle N)^{-1} \sum_l (\cdot)$ is an average over edges. Writing $\sum_l (\cdot) = \sum_{ij} \hat{a}_{ij}(\cdot)$, r can be expressed as [17]

$$r = \frac{\langle k \rangle \langle k^2 \overline{k_{nn}}(k) \rangle - \langle k^2 \rangle^2}{\langle k \rangle \langle k^3 \rangle - \langle k^2 \rangle^2}. \quad (7)$$

In the infinite network-size limit we expect $r = 0$ in the configuration model (null model) as there are no built in correlations. Even if the index r is widely used to measure network correlations, some drawbacks of it have been put forward [18, 19]

Results

Emergence of effective correlations in finite-size networks

We have computationally constructed finite random networks with different degree distributions; in particular, Poissonian, Gaussian, and scale-free distributions, assembled using the configuration model as explained above (for the scale-free case see Ref. [20]) and measured their Pearson's correlation coefficient. Results are illustrated in Fig.2; the probability of obtaining negative (disassortative) values of r is larger than the one for positive (assortative) values (observe the shift between $r = 0$ and the curve averaged value). This means that the null-model expectation value of r is negative! i.e. finite random networks are more likely to be disassortative than assortative. This result is highly counterintuitive because the ensemble is constructed without assuming any type of correlations and is, clearly, a finite-size effect. Indeed, for larger network sizes the averaged value of r converges to 0 as we have analytically proved and computationally verified. For instance, for scale-free networks, r can be easily shown to converge to 0 as $r \propto N^{-1/3}$ in the large- N limit (see Appendix B and Fig.2B). A well-known effect leading to effective disassortativity, is that simple algorithms, which are supposed to generate uncorrelated networks, can instead lead to degree-degree anti-correlations when the desired degree distribution has a heavy tail and no more than one link is allowed between any two vertices (as hubs are not as connected among themselves as they should be without such a constraint) [21, 22]. Also, our observation is in agreement with the recent claim that, owing to entropic effects, real scale-free networks are typically disassortative: simply, there are many more ways to wire networks with disassortative correlations than with assortative ones [23].

Effective correlations imply nestedness in finite networks

A straightforward consequence of the natural tendency of finite networks to be disassortative is that they thereby also become naturally nested. Indeed, the nestedness index η was defined assuming there were no built-in correlations, but if degree-degree correlations effectively emerge in finite-size random networks, then deviations from the neutral value $\eta = 1$ are to be expected. Indeed, in Fig.2C we have considered networks constructed with the configuration model, employing the same probability distributions (Gaussian, Poissonian and scale free) as above. For each so-constructed random network we compute both r and η and plot the average of the second as a function of the first (technical details on how to sample networks with extreme values of r –using the Wang-Landau algorithm [24]– are given in Appendix D). The resulting three curves exhibit a neat (almost linear) dependence of the expected value of η on r : disassortative networks are nested while assortative ones are anti-nested. As disassortative ones are more likely to appear, a certain degree of nestedness is to be expected in finite random networks. Observe that for truly uncorrelated random networks, i.e. with $r = 0$, the expectation value of η is 1.

Finally, in Appendix C, we provide an analytical connection between disassortativity and nestedness in random networks with explicitly built-in degree-degree correlations. Also in this case a clear relation between nestedness and disassortativity emerges (as shown in the figure of appendix C) for scale-free networks.

Degree correlations in real vs randomized networks

We have considered 60 different empirical networks, both bipartite and unimodal, from the literature. The set includes foodwebs, metabolic, neuronal, ecological, social, and technological networks (see Table 1 and 2). We have performed randomizations preserving the corresponding degree sequences (configuration ensemble) and avoiding multiple links between any pair of nodes. Results for a subset of 16 networks are illustrated in Figure 3, which shows the distribution of r -values (see figure caption) compared with the actual value of r .

The actual value of r in empirical networks coincides with the ensemble average within an error of the order of 1, 2, or 3 standard deviations in about two thirds of the cases (53%, 67%, and 76% respectively). Similarly, the corresponding p-values are larger than the significance threshold (0.05) in 60% of the cases. Particularizing for bipartite networks, the z-scores rise to: 60%, 76%, and 89%, respectively, and the significant P-values go up to 68% (data are collected in Table 1 and 2).

Therefore, roughly speaking, the null model –in which networks are randomly wired according to a specified degree sequence– explains well the correlations of about two-thirds (or more) of the networks we have analysed and, more remarkably, it explains even better the correlations of bipartite networks. Thus, once it has been realized that random networks have a slight natural tendency to be disassortative, in many cases, there does not seem to be a clear generic statistical tendency for real networks to be more correlated (either assortatively or disassortatively) than expected in the null model. For instance in almost all foodwebs we have analyzed the empirical value of r is well explained by randomizations, while in some other social and biological networks there are some residual positive correlations (assortativity).

Nestedness in real vs randomized networks

We have conducted a similar analysis for the nestedness index η and compare its value in real networks with the expected value in randomizations (see Fig.3). In this case, the actual value of η in empirical networks coincides with the ensemble average with an error of the order of 1, 2, or 3 standard deviations also in about two thirds of the cases (43%, 73%, and 83% respectively). As for the p-value, it is above threshold in 63% of the cases (which goes up to 76% for bipartite networks). Thus, in most of the analysed examples, empirically observed values of nestedness are in agreement with null-model expectations once the degree-distribution has been taken into consideration (data shown in Table 1 and Table 2).

Nestedness vs degree correlations in empirical networks

As said above, both Fig.2C and Fig.3 reveal a global tendency: exceedingly disassortative empirical networks tend to be nested while assortative ones are anti-nested. To further explore this relation, Fig.4 shows a plot of nestedness against assortativity for the selection of empirical networks listed in Table 1 and Table 2. Although these networks are highly disparate as regards size, density, degree distribution, etc., it is apparent that the main contribution to η comes indeed from degree-degree correlations. *The observation of such a strong generic correlation between the nestedness and disassortativity constitutes one of the main findings of this paper.*

A more refined null model

A unique criterion for choosing a proper null model does not exist [25]. For instance, it is possible to go beyond the null model studied so far by preserving not just the degree sequence but also empirical correlations. Indeed, from the full set of networks generated with the configuration model for a given degree sequence, one could consider the subset of networks with a fixed value of r , as done in Fig.2C (and as explained in Appendix C). In particular, one could take the sub-ensemble with the same r as empirically observed. This constitutes a more refined null model in which the number of nodes, degree sequence, and degree-degree correlations are preserved. This more refined null model reproduces slightly better than the configuration model the empirical values of nestedness; for instance, allowing for three standard deviations bipartite networks are explained in a 100% of the cases (details can be found in Appendix D). Thus, the null model preserving degree-degree correlations explains quite well the observed levels of nestedness.

Discussion and Conclusions

Theoretical studies suggest that a nested structure minimizes competition and increases the number of coexisting species [13], and also it makes the community more robust to random extinctions [26] and habitat loss [27]. In order to make progress, systematic analyses of nestedness and nestedness indices are necessary.

The first contribution of this work is that a new analytical nestedness index has been introduced. It is a variant of the one introduced in Ref. [13], allowing for analytical developments, which are not feasible with standard computational estimators (or calculators) of nestedness. Besides that, the new index exhibits a number of additional advantages: (i) it allows us to

identify the amount of nestedness associated with each single node in a network, making it possible to define a “local nestedness”; (ii) the new index is properly normalized and provides an output equal to unity in uncorrelated random networks, allowing us in this way to discriminate contributions to nestedness beyond network heterogeneity.

Having removed the direct effects of the degree distribution –which has a dominant contribution to other measures of nestedness– it is possible to move one step forward and ask how degree-degree correlations (as quantified by Pearson’s coefficient) influence nestedness measurements. Curiously enough, there are more disassortative (negatively degree-degree correlated) networks than assortative ones even among randomly assembled networks. Different reasons for this have already been pointed out in the literature [21–23] and we have confirmed that indeed this is the case for finite networks built with the configuration model.

Therefore, the neutral expectation for finite random networks is to have some non-vanishing level of disassortativity ($r < 0$). Analogously, as we have first reported here, there is a very similar tendency for finite random networks to be naturally nested. There is a clean-cut correspondence between nestedness and disassortativity: disassortative networks are typically nested and nested networks are typically disassortative. This is true for finite-size computational random models, analytically studied correlated networks of any size (Appendix C), as well as in real empirical networks (as vividly illustrated in Figure 2C and Fig.4).

Analyses of 60 empirical networks (both bipartite and non-bipartite) taken from the literature reveal that in many cases the measured nestedness is in good correspondence with that of the degree-preserving null model. In particular, almost 90% of the studied bipartite networks are well described by the null model and this figure rises up to 100% when a more refined null model is considered. Finally, recent results by Allesina’s group [15] suggest that one should consider weighted networks to properly study nestedness; we leave an extension of our analyses along this line for a future work.

In conclusion, degree heterogeneity together with the finite size of real networks suffice to justify most of the empirically observed levels of nestedness in ecological bipartite network.

Acknowledgments: We are especially grateful to J.A. Dunne for providing us with food-web data, and to A. Arenas and M. Newman for making the other network data available online. Many thanks also to A. Pascual-García and P. Moretti for fruitful conversations.

References

1. Barabási A (2002) *Linked: The New Science of Networks*. Perseus Books Group.
2. Albert R, Barabási A (2002) Statistical mechanics of complex networks. *Rev Mod Phys* 74: 47–97.
3. Newman M (2003) The structure and function on complex networks. *SIAM Reviews* 45: 167.
4. Boccaletti S, Latora V, Moreno Y, Chavez M, Hwang D (2006) Complex networks: Structure and dynamics. *Phys Rep* 424: 175.

5. Barrat A, Barthelemy M, Vespignani A (2008) *Dynamical processes on complex networks*. Cambridge: Cambridge University Press.
6. May RM (1972) Will a large complex system be stable? *Nature* 238: 413.
7. Allesina S, Tang S (2012) Stability criteria for complex ecosystems. *Nature* 483: 205-208.
8. Atmar W, Paterson BD (1993) The measure of order and disorder in the distribution of species in fragmented habitat. *Oecologia* 96: 373-382.
9. Wright DH, Reeves JH (1992) On the meaning and measurement of nestedness of species assemblages. *OECOLOGIA* 92: 414-428.
10. Fischer J, Lindenmayer D (2002) Treating the nestedness temperature calculator as a "black box" can lead to false conclusions. *Oikos* 99: 193-199.
11. Ulrich W, Almeida-Neto M, Gotelli NJ (2009) A consumer's guide to nestedness analysis. *Oikos* 118: 3-17.
12. Bascompte J, Jordano P, Melián CJ, Olesen JM (2003) The nested assembly of plant animal mutualistic networks. *Proc Nat Acad Sci* 100: 9383-9387.
13. Bastolla U, Fortuna M, Pascual-García A, Ferrera A, Luque B, et al. (2009) The architecture of mutualistic networks minimizes competition and increases biodiversity. *Nature* 458: 1018-21.
14. Sugihara G, Ye H (2009) Cooperative network dynamics. *Nature* 458: 979.
15. Staniczenko PPA, Kopp J, Allesina S (2013) The ghost of nestedness in ecological networks. *Nature Communications* 4: 139.
16. Molloy M, Reed B (1995) A critical point for random graphs with a given degree sequence. *Random Structures and Algorithms* 6: 161-180.
17. Newman M (2002) Mixing patterns in networks. *Phys Rev Lett* 89: 208701.
18. Dorogovtsev SN, Ferreira AL, Goltsev AV, Mendes JFF (2002) Zero pearson coefficient for strongly correlated growing tree network. *Physical Review E* 81: 031135.
19. Xu X, Zhang J, Sun J, Small M (2009) Revising the simple measures of assortativity in complex networks. *Physical Review E* 80: 056106.
20. Catanzaro M, Boguña M, Pastor-Satorras R (2005) Generation of uncorrelated random scale-free networks. *Phys Rev E* 71: 027103.
21. Maslov S, Sneppen K, Zaliznyak A (2004) Detection of topological patterns in complex networks: Correlation profile of the internet. *Physica A* 333: 529-540.
22. Park J, Newman M (2003) The origin of degree correlations in the internet and other networks. *Phys Rev E* 66: 026112.

23. Johnson S, Torres J, Marro J, Muñoz M (2010) Entropic origin of disassortativity in complex networks. *Phys Rev Lett* 104: 108702.
24. Wang F, Landau D (2001) Efficient multiple-range random walk algorithm to calculate the density of states. *Physical Review Letters* 86: 2050-2053.
25. Gotelli N (2001) Research frontiers in null model analysis. *Global Ecology and Biogeography* 10: 337–343.
26. Burgos E, Ceva H, Perazzo RP, Devoto M, Medan D, et al. (2007) Why nestedness in mutualistic networks? *Journal of Theoretical Biology* 249: 307–313.
27. Fortuna M, Bascompte J (2006) Habitat loss and the structure of plant– animal mutualistic networks. *Ecology Letters* 9: 281–286.
28. Capocci A, Caldarelli G, de los Rios P (2003) Quantitative description and modeling of real networks. *Phys Rev E* 68: 047101.
29. Pastor-Satorras R, Vázquez A, Vespignani A (2001) Dynamical and correlation properties of the internet. *Phys Rev Lett* 87: 258701.
30. Harriger L, van den Heuvel MP, Sporns O (2012) Rich club organization of macaque cerebral cortex and its role in network communication. *Plos One* 7: e46497.
31. Duch J, Arenas A (2005) Community identification using extremal optimization. *Physical Review E* 72: 027104.
32. Watts DJ, Strogatz SH (1998) Collective dynamics of 'small-world' networks. *Nature* 393: 440-442.
33. Jeong H, Mason S, Barabási A, Oltvai ZN (2001) Centrality and lethality of protein networks. *Nature* 411: 41.
34. McAuley J, Leskovec J (2012) Learning to discover social circles in ego networks. In: *Advances in Neural Information Processing Systems*. pp. 548–556.
35. Zachary WW (1977) An information flow model for conflict and fission in small groups. *Journal of Anthropological Research* 33: 452-473.
36. Kaitiaki trust network. available at <http://www.trustlet.org/datasets/kaitiaki/> .
37. Adamic LA, Glance N (2005) The political blogosphere and the 2004 us election. *Proceedings of the WWW-2005 Workshop on the Weblogging Ecosystem* .
38. Norlen K, Lucas G, Gebbie M, Chuang J (2002) Eva: Extraction, visualization and analysis of the telecommunications and media ownership network. *Proceedings of International Telecommunications Society 14th Biennial Conference, Seoul Korea* .
39. Cross R, Parker A (2004) *The Hidden Power of Social Networks*. Boston: Harvard Business School Press.

40. Lusseau D, Schneider K, Boisseau OJ, Haase P, Slooten E, et al. (2003) The bottlenose dolphin community of doubtful sound features a large proportion of long-lasting associations. *Behavioral Ecology and Sociobiology* 54: 396-405.
41. P Gleiser, Danon L (2003) Community structure in jazz. *Adv Complex Syst* 6: 565.
42. Girvan M, Newman MEJ (2002) Community structure in social and biological networks. *Proc Natl Acad Sci USA* 99: 7821-1826.
43. Newman MEJ (2006) Finding community structure in networks using the eigenvectors of matrices. *Phys Rev E* 74: 036104.
44. Opsahl T (2011) Why anchorage is not (that) important: Binary ties and sample selection. Available at <http://wpme/poFcY-Vw> .
45. Watts DJ, Strogatz SH (1998) Collective dynamics of 'small-world' networks. *Nature* 393: 440-442.
46. Opsahl T, Agneessens F, Skvoretz J (2010) Node centrality in weighted networks: Generalizing degree and shortest paths. *Social Networks* 3: 245-251.
47. Arroyo MTK, Primack RB, , Armesto JJ (1982) Community studies in pollination ecology in the high temperate andes of central chile. i. pollination mechanisms and altitudinal variation. *American Journal of Botany* 69: 82-97.
48. Clements RE, Long FL (1923) *Experimental pollination. An outline of the ecology of flowers and insects.* Washington D.C., USA: Carnegie Institute of Washington.
49. Dupont Y, Hansen D, Olesen J (2003) Structure of a plant-flower-visitor network in the high-altitude sub-alpine desert of tenerife, canary islands. *Ecography* 26: 301-310.
50. Hocking B (1968) Insect-flower associations in the high arctic with special reference to nectar. *Oikos* 19: 359-388.
51. McCullen CK (1993) Flower-visiting insects of the galapagos islands. *Pan-Pacific Entomologist* 69: 95-106.
52. Medan D, Montaldo NH, Devoto M, Mantese A, Vasellati V, et al. (2002) Plant-pollinator relationships at two altitudes in the andes of mendoza, argentina. *Arctic Antarctic and Alpine Research* 34: 233-24.
53. Ramirez N, Brito Y (1992) Pollination biology in a palm swamp community in the venezuelan central plains. *Botanical Journal of the Linnean Society* 110: 277-302.
54. Barrett SCH, Helenurm K (1987) The reproductive-biology of boreal forest herbs.1. breeding systems and pollination. *Canadian Journal of Botany* 65: 2036-2046.
55. Elberling H, Olesen JM (1999) The structure of a high latitude plant-flower visitor system: the dominance of flies. *Ecography* 22: 314-323.

56. Kevan PG (1970) High arctic insect-flower visitor relations: the inter-relationships of arthropods and flowers at Lake Hazen, Ellesmere Island, Northwest Territories, Canada. Ph.D. thesis, University of Alberta.
57. Memmott J (1999) The structure of a plant-pollinator food web. *Ecology Letters* 2: 276-280.
58. Mosquin T, Martin JEH (1967) Observations on the pollination biology of plants on melville island, n.w.t., canada. *Canadian Field Naturalist* 81: 201-205.
59. Motten AF (1982) Pollination Ecology of the Spring Wildflower Community in the Deciduous Forests of Piedmont North Carolina. North Carolina, USA: Doctoral Dissertation thesis, Duke University, Durham.
60. Olesen JM, Eskildsen LI, Venkatasamy S (2002) Invasion of pollination networks on oceanic islands: importance of invader complexes and endemic super generalists. *Diversity and Distributions* 8: 181-192.
61. Ollerton J, Johnson SD, Cranmer L, Kellie S (2003) The pollination ecology of an assemblage of grassland asclepiads in south africa. *Annals of Botany* 92: 807-834.
62. Schemske DW, Willson MF, Melampy MN, Miller LJ, Verner L, et al. (1978) Flowering ecology of some spring woodland herbs. *Ecology* 59: 351-366.
63. Inouye DW, Pyke GH (1988) Pollination biology in the snowy mountains of australia: comparisons with montane colorado, usa. *Australian Journal of Ecology* 13.
64. Small E (1976) Insect pollinators of the mer bleue peat bog of ottawa. *Canadian Field Naturalist* 90: 22-28.
65. Vázquez DP (2002) Interactions among Introduced Ungulates, Plants, and Pollinators: A Field Study in the Temperate Forest of the Southern Andes. Doctoral Dissertation thesis. Knoxville, Tennessee, USA: University of Tennessee, USA.
66. Vázquez DP, Simberloff D (2002) Ecological specialization and susceptibility to disturbance: conjectures and refutations. *American Naturalist* 159: 606-623.
67. Vázquez DP, Simberloff D (2003) Changes in interaction biodiversity induced by an introduced ungulate. *Ecology Letters* 6: 1077-1083.
68. Joern A (1979) Feeding patterns in grasshoppers (orthoptera: Acrididae): factors influencing diet specialization. *Oecologia* 38: 325-347.
69. Leather S (1991) Feeding specialisation and host distribution of british and finnish prunus feeding macrolepidoptera. *OIKOS* 60: 40-48.
70. Beehler B (1983) Frugivory and polygamy in birds of paradise. *The Auk* 100: 1-12.

71. Poulin B, Wright SJ, Lefebvre G, Calderon O (1999) Interspecific synchrony and asynchrony in the fruiting phenologies of congeneric bird-dispersed plants in panama. *Journal of Tropical Ecology* 15: 213-227.
72. Snow BK, Snow DW (1971) The feeding ecology of tanagers and honeycreepers in trinidad. *The Auk* 88: 291-322.
73. Sorensen A (1981) Interactions between birds and fruit in a temperate woodland. *Oecologia* 50: 242-249.
74. Ollerton J, McCollin D, Fautin D, Allen G (2006) Finding nemo: nestedness engendered by mutualistic organisation in anemonefish and their hosts. *Proceedings of the Royal Society B* : doi:10.1098.

Appendix A: Nestedness index for bipartite networks

Mutualistic networks are usually bipartite: two sets of nodes exist such that all edges are between nodes in one set and those of another. The ones considered in Ref. [13], for instance, are composed of animals and plants which interact in symbiotic relations of feeding-pollination; these interactions only take place between animals and plants. Let us therefore consider a bipartite network and call the sets Γ_1 and Γ_2 , with n_1 and n_2 nodes, respectively ($n_1 + n_2 = N$). Using the notation $\langle \cdot \rangle_i$ for averages over set Γ_i , the total number of edges is $\langle k \rangle_1 n_2 = \langle k \rangle_2 n_1 = \frac{1}{2} \langle k \rangle N$. Assuming that the network is defined by the configuration ensemble, though with the additional constraint of being bipartite, the probability of node l being connected to node i is

$$\hat{e}_{il} = 2 \frac{k_i k_l}{\langle k \rangle N}$$

if they belong to different sets, and zero if they are in the same one. Proceeding as before, we find that the expected value of the nestedness for a bipartite network is

$$\eta_{bip} = \frac{1}{N^2} \left[\sum_{i,j \in \Gamma_1} \frac{1}{k_i k_j} \sum_{l \in \Gamma_2} \frac{k_i k_l}{\langle k \rangle_1 n_2} \frac{k_l k_j}{\langle k \rangle_2 n_1} + \sum_{i,j \in \Gamma_2} \frac{1}{k_i k_j} \sum_{l \in \Gamma_1} \frac{k_i k_l}{\langle k \rangle_1 n_2} \frac{k_l k_j}{\langle k \rangle_2 n_1} \right] = \frac{n_1 \langle k^2 \rangle_2 + n_2 \langle k^2 \rangle_1}{\langle k \rangle_1 \langle k \rangle_2 (n_1 + n_2)^2}. \quad (8)$$

Interestingly, if $n_1 = n_2$, the fact that the network is bipartite has no effect on the nestedness: $\eta_{bip} = \eta_{conf}$.

Appendix B: Finite Size Scaling of Pearson's coefficient in scale-free networks

As show in Fig.2, finite-size networks built with the configuration model have a non-vanishing value of Pearson's coefficient, r . Given the fact that these networks are constructed without assuming any type of correlations, this is necessarily a finite-size effect. Let us compute r explicitly in finite-size scale-free networks, with $P(k) \propto k^{-\gamma}$ with $2 < \gamma < 3$. The maximum expected degree, k in a network of size N is of the order $N^{\frac{1}{\gamma-1}}$ and this cut-off controls the scaling of moments $\langle k^m \rangle \sim \int_1^{K_{max}} k^m k^{-\gamma} dk \sim k^{m-\gamma+1} \Big|_1^N \sim N^{\frac{m-\gamma+1}{\gamma-1}} - 1$. Combining the expressions for the first three moments appearing in the definition of r , Eq.7, one readily obtains;

$$r = \frac{aN^{\frac{3-\gamma}{\gamma-1}} - bN^{2\frac{3-\gamma}{\gamma-1}}}{cN^{\frac{4-\gamma}{\gamma-1}} - dN^{2\frac{3-\gamma}{\gamma-1}}} \sim -eN^{\frac{2-\gamma}{\gamma-1}} \quad (9)$$

where a, b, c, d , and e are un-specified positive constants. For a scale-free network with $\gamma = 2.5$ this reduces to $r \sim N^{-\frac{1}{3}}$ in agreement with numerical results shown in Fig.2 (observe that, as we use a logarithmic scale, the absolute value of r rather than r itself is employed).

Appendix C: Degree-degree correlations in heterogeneous networks

It has been recently shown [23] that there is a mapping between any mean-nearest-neighbour function $\overline{k_{nn}}(k)$ –accounting for degree-degree correlations– and its corresponding mean-adjacency-matrix \hat{e} , which is as follows:

$$\overline{k_{nn}}(k) = \frac{\langle k^2 \rangle}{\langle k \rangle} + \int d\nu f(\nu) \sigma_{\nu+1} \left[\frac{k^{\nu-1}}{\langle k^\nu \rangle} - \frac{1}{k} \right]. \quad (10)$$

This can be seen as an expansion of $\overline{k_{nn}}(k)$ in powers of k with some weight function f and $\sigma_{\nu+1} \equiv \langle k^{\nu+1} \rangle - \langle k \rangle \langle k^\nu \rangle$ (which can always be done [23]), the corresponding matrix \hat{e} takes the form

$$\hat{e}_{ij} = \frac{k_i k_j}{\langle k \rangle N} + \int d\nu \frac{f(\nu)}{N} \left[\frac{(k_i k_j)^\nu}{\langle k^\nu \rangle} - k_i^\nu - k_j^\nu + \langle k^\nu \rangle \right]. \quad (11)$$

Without entering here the details of this decomposition (for which we refer the reader to Ref. [23]) let us just remark that the first term in Eq.(11) coincides with the expected value for the standard configuration model, while the second one accounts for correlations. Hence, Eq.(11) can be seen as an extension of the configuration model including correlations, i.e. a *correlated configuration model*. In particular, Eq.(11) encodes the way a network should be wired (i.e. the probabilities with which any pair of nodes should be connected) to have the desired degree sequence and degree-degree correlations.

In many empirical scale-free networks, $\overline{k_{nn}}(k)$ can be fitted by $\overline{k_{nn}}(k) = A + Bk^\beta$, with $A, B > 0$ [4, 28, 29] – the mixing being assortative (disassortative) if β is positive (negative). Such a case is described by Eq. (10) with $f(\nu) = C[\delta(\nu - \beta - 1)\sigma_2/\sigma_{\beta+2} - \delta(\nu - 1)]$, with C a positive constant, which simplifies significantly the expressions above. This choice yields

$$\overline{k_{nn}}(k) = \frac{\langle k^2 \rangle}{\langle k \rangle} + C\sigma_2 \left[\frac{k^\beta}{\langle k^{\beta+1} \rangle} - \frac{1}{\langle k \rangle} \right] \quad (12)$$

After plugging Eq. (12) into Eq. (7), one obtains:

$$r = \frac{C\sigma_2}{\langle k^{\beta+1} \rangle} \left(\frac{\langle k \rangle \langle k^{\beta+2} \rangle - \langle k^2 \rangle \langle k^{\beta+1} \rangle}{\langle k \rangle \langle k^3 \rangle - \langle k^2 \rangle^2} \right). \quad (13)$$

It turns out that the configurations most likely to arise naturally (i.e those with maximal entropy) usually have $C \simeq 1$ [23]. Therefore, and for the sake of analytical simplicity, we shall consider this particular case³; that is, we shall use

$$\hat{e}_{ij} = \frac{1}{N} \left\{ \frac{\sigma_2}{\sigma_{\beta+2}} \left[\frac{(k_i k_j)^{\beta+1}}{\langle k^{\beta+1} \rangle} - k_i^{\beta+1} - k_j^{\beta+1} + \langle k^{\beta+1} \rangle \right] + k_i + k_j - \langle k \rangle \right\}. \quad (14)$$

³Note that $C = 1$ corresponds to removing the linear term, proportional to $k_i k_j$, in Eq. (11), and leaving the leading non-linearity, $(k_i k_j)^{\beta+1}$, as the dominant one.

Substituting the adjacency matrix for this expression in the definition of η (Eq.6), we obtain its expected value as a function of the remaining parameter β :

$$\bar{\eta}(\beta) = \frac{\langle k \rangle^2}{\langle k^2 \rangle} \left[1 + (\sigma_2 - \alpha_\beta^2 \rho_\beta) \left(2 \frac{\langle k^\beta \rangle \langle k^{-1} \rangle}{\langle k^{\beta+1} \rangle} - \langle k^{-1} \rangle^2 \right) + \alpha_\beta^2 \rho_\beta \left(\frac{\langle k^\beta \rangle}{\langle k^{\beta+1} \rangle} \right)^2 \right],$$

where $\alpha_\beta \equiv \sigma_2 / \sigma_{\beta+2}$ and $\rho_\beta \equiv \langle k^{2(\beta+1)} \rangle - \langle k \rangle^{2(\beta+1)}$. Note that $\bar{\eta}_0 = 1$, as corresponds to uncorrelated networks.

As r can be inferred from β using Eq.(13), then we can plot the resulting η as a function of r for different networks. In particular, for scale-free networks with $P(k) \sim k^{-\gamma}$ we obtain the curves shown in Fig.A1; they exhibit a clear tendency (at least for $\gamma > 2$): disassortative networks tend to be nested and the or the way around.

Appendix D: Sampling networks with a given value of r

Given that networks with very large r (in absolute value) are rare, and thus they seldom appear in the randomization process used to build the configurational ensemble (or null model) we have implemented the Wang-Landau (multi-canonical) algorithm to enrich the sampling with such rare networks [24]. The gist of this technique is to perform a “random” walk in the r -space, in such a way that jumps toward frequently visited r -values are penalized and, instead, rarely visited r 's are favoured, which requires storing the statistics of the number of times every value of r has been previously “extracted”. Starting from an initial network (with r_1), a small change in its topology is tentatively made, and the resulting new network (with r_2) is accepted with probability

$$P(r_1 \rightarrow r_2) = \min \left[\frac{g(r_1)}{g(r_2)}, 1 \right] \quad (15)$$

where $g(r)$ stands for the (previously observed) frequency. This algorithm allows for uniform searches in “ r -space”.

For the three different types of degree-distributions considered above, we proceed as follows:

- Generate a network ($N = 50$) with the configuration model with a fixed degree sequence.
- Explore the r -space using the Wang-Landau algorithm (up to, at least, 4000 different visits to the most frequent states).
- Average over 500 independent realizations.

While running the search in the r -space, we also measure and store the nestedness values of Eq. 6 for every (binned) value of r ; after properly normalizing, we obtain the averaged value of nestedness as a function of r as shown in Fig.2.

In all three cases, we obtain a very clear (almost linear) dependence between r and η : disassortative networks are distinctly nested (on average) while assortative ones are anti-nested (on average). Let us caution that this conclusion holds “on average”, i.e. our results do not necessarily imply that any particular disassortative network is actually nested.

For the case of scale free networks we have been able to analytically determine the relation between the averaged Pearson’s coefficient and the averaged nestedness. Results are illustrated in Figure A1, which shows the value of $\bar{\eta}_\beta$ (given by Eq. (15) in Appendix A) against the assortativity r for various scale-free networks. Nestedness is seen to grow very fast with increasing disassortativity (decreasing negative r), while in general slightly assortative networks are less nested than neutral (uncorrelated) ones, i.e. they are “anti-nested”. Note, however, that highly heterogeneous networks (scale-free with $\gamma \rightarrow 2$) show an increase in $\bar{\eta}_\beta$ for large positive r .

Analogously to what was done for the configuration model, we compute the average nestedness in this second ensemble for a fixed value of r . In particular, we have considered the same 16 workbench networks as above, and produced Figure A2, where we show for each network, the averaged nestedness (with its corresponding standard deviation) as a function of r . The empirical values of r, η are marked with black crosses.

In this new, more constrained ensemble the null model performs only slightly better than the configurational one: 63% within one standard deviation (as opposed to 42% in the first null model), 85% within two (versus 72%), and 92% for three standard deviations (as opposed to 82%). Observe that, also here, empirical values are reasonably well explained by randomized values, in almost all cases.

Appendix E: Network Data

Unimodal networks on Fig 4

Network	r	r z-score	r P-value	η	η z-score	η P-value	η z-score with correlations
Biological - Food Webs (13)							
Little Rock lake	-0.327	0.514 ()	0.300 ()	1.326	0.026 ()	0.199 ()	0.350 ()
Ythan Estuary	-0.278	2.000 ()	0.039 (*)	1.482	-2.459 ()	0.021 (*)	-1.339 ()
Stony Stream	-0.208	0.368 ()	0.401 ()	1.295	-0.500 ()	0.300 ()	-0.594 ()
Canton creek	-0.201	0.667 ()	0.266 ()	1.331	-1.454 ()	0.096 ()	-0.880 ()
Skipwith Pond	-0.086	-3.406 (*)	0.001 (*)	1.014	2.142 ()	0.017 (*)	-4.600 (*)
El Verde rainforest	-0.171	0.133 ()	0.306 ()	1.187	1.520 ()	0.072 ()	0.561 ()
Caribbean Reef	-0.164	-0.778 ()	0.245 ()	1.095	-0.687 ()	0.297 ()	-3.140 (*)
St. Martin Island	-0.135	0.723 ()	0.226 ()	1.181	-3.000 ()	0.005 (*)	-5.488 (*)
UK grassland	-0.182	1.093 ()	0.142 ()	1.266	-1.412 ()	0.069 ()	-0.985 ()
Chesapeake bay	-0.115	-0.510 ()	0.299 ()	1.080	1.015 ()	0.162 ()	1.191 ()
Northwest Shelf	-0.082	-5.125 (*)	0.000 (*)	1.024	5.000 (*)	0.001 (*)	-0.495 ()
Coachella Valley	0.050	-4.548 (*)	0.000 (*)	0.990	4.272 (*)	0.000 (*)	0.031 ()
St. Marks Forest	0.116	-3.379 (*)	0.000 (*)	0.984	2.733 ()	0.002 (*)	-0.205 ()
Biological - other (4)							
Macaque cortex [30]	-0.295	-3.167 (*)	0.001 (*)	1.664	0.076 ()	0.484 ()	-2.909 ()
C.elegans metabolic network [31]	-0.220	4.434 (*)	0.001 (*)	1.736	-1.500 ()	0.166 ()	0.5 ()
C.elegans neuronal connectivity [32]	-0.163	7.443 (*)	0.000 (*)	1.908	-12.446 (*)	0.000 (*)	-3.875 (*)
Yeast metabolic [33]	-0.076	-	-	1.411	-	-	-
Social (12)							
Facebook friendship [34]	-0.712	-	-	4.077	-	-	-
Karate club [35]	-0.476	3.744 (*)	0.000 (*)	1.568	-3.487 (*)	0.000 (*)	-0.303 ()
Kaitiaki web relations [36]	-0.245	1.698 (*)	0.042 (*)	0.203	-0.904 ()	0.165 ()	0.287 ()
Political blogs [37]	-0.221	-	-	1.549	-	-	-
Ownership network [38]	-0.181	-	-	2.315	-	-	-
Consulting firm [39]	-0.167	-	-	1.073	-	-	-
Political books in th US [37]	-0.128	-0.622 ()	0.229 ()	1.103	0.800 ()	0.189 ()	0.919 ()
Dolphins relationships [40]	-0.044	0.149 ()	0.460 ()	1.164	-1.020 ()	0.157 ()	-1.480 ()
Jazz musicians [41]	0.020	-7.000 (*)	0.000 (*)	0.997	4.631 (*)	0.000 (*)	1.631 ()

Football games [42]	0.162	-4.526 (*)	0.000 (*)	0.999	2.000 ()	0.002 (*)	-3.832 (*)
Net-science arXiv [43]	0.462	-	-	0.653	-	-	-
Technical (3)							
Airports network [44]	-0.221	-	-	2.352	-	-	-
Power grid [45]	0.003	-	-	1.198	-	-	-
World flights [46]	0.051	-	-	1.134	-	-	-

Table 1. Empirical (unimodal) networks from different backgrounds appearing in Fig.4 and their values of Pearson’s correlation coefficient and nestedness η . The z-score and P-values are calculated with respect to the random null model, and the “z-score with correlations” with the null model constraint to keep to the actual value of the Pearson’s coefficient r . The asterisks * stand for z-values larger than 3 (in absolute value) and P-values smaller than the threshold 0.05.

Empirical bipartite networks on Fig 4

Network	r	r z-score	r P-value	η	η z-score	η P-value	η z-score with correlations
Plant - Pollinator (28)							
Andean scrub (1) (Chile) [47]	-0.239	2.448 ()	0.009 (*)	1.409	-2.857 ()	0.005 (*)	-1.067 ()
Andean scrub (2) (Chile) [47]	-0.363	2.840 ()	0.003 (*)	1.208	-3.246 (*)	0.001 (*)	-1.595 ()
Montane forest and grassland (USA) [48]	-0.131	-2.364 ()	0.011 (*)	1.218	1.067 ()	0.131 ()	-0.442 ()
High-altitude desert (Canary Islands) [49]	-0.018	0.625 ()	0.253 ()	0.989	-0.340 ()	0.334 ()	0.397 ()
Arctic community (Canada) [50]	-0.128	1.467 ()	0.079 ()	1.246	-1.164 ()	0.116 ()	0.195 ()
Multiple Communities (Galápagos Islands) [51]	-0.638	5.444 (*)	0.000 (*)	2.416	-5.033 (*)	0.003 (*)	-1.957 ()
Xeric scrub (Argentina) [52]	-0.241	4.086 (*)	0.000 (*)	1.447	-4.104 (*)	0.000 (*)	-0.919 ()
Woody riverine veg. and xeric scrub (Argentina) [52]	-0.124	0.722 ()	0.224 ()	1.268	-1.550 ()	0.071 ()	-1.745 ()
Palm swamp community (Venezuela) [53]	-0.074	0.018 ()	0.492 ()	0.872	0.370 ()	0.382 ()	1.033 ()
Boreal forest (Canada) [54]	-0.069	1.815 ()	0.030 (*)	1.309	-0.926 ()	0.138 ()	-0.151 ()
Alpine subarctic community (sweden) [55]	-0.034	0.500 ()	0.298 ()	1.061	-0.500 ()	0.282 ()	-0.625 ()
High Arctic (Canada) [56]	-0.075	0.875 ()	0.171 ()	1.322	-2.866 ()	0.030 (*)	-2.977 ()
Medow (U.K) [57]	-0.104	0.049 ()	0.434 ()	1.442	-1.049 ()	0.156 ()	-0.658 ()
Arctic community (Canada) [58]	-0.104	-1.720 ()	0.031 (*)	0.821	1.472 ()	0.069 ()	-0.485 ()
Deciduous forest (USA) [59]	-0.040	-0.571 ()	0.307 ()	1.130	0.544 ()	0.297 ()	0.130 ()
Coastal forest (Mauritius Island) [60]	-0.488	2.278 ()	0.020 (*)	1.257	-3.378 (*)	0.002 (*)	-2.143 ()
Upland grassland (South Africa) [61]	-0.041	-1.000 ()	0.180 ()	1.180	0.885 ()	0.232 ()	0.017 ()
Maple-oak woodland (USA) [62]	-0.037	0.500 ()	0.320 ()	1.114	-0.166 ()	0.426 ()	0.578 ()
Snowy Mountains of Australia [63]	-0.139	0.778 ()	0.236 ()	1.165	-1.432 ()	0.076 ()	-0.804 ()
Peat bog (Canada) [64]	0.003	-2.857 ()	0.002 (*)	0.905	1.722 ()	0.035 (*)	-0.367 ()
Arroyo Goye (Argentina) [65-67]	-0.034	-0.091 ()	0.497 ()	0.114	-0.125 ()	0.446 ()	-0.507 ()
Cerro Lopez (Argentina) [65-67]	-0.030	0.071 ()	0.412 ()	0.133	-0.250 ()	0.352 ()	-0.078 ()
Llao Llao (Argentina) [65-67]	-0.059	0.182 ()	0.375 ()	0.124	-0.375 ()	0.317 ()	-0.504 ()
Mascardi (c) (Argentina) [65-67]	-0.034	0.500 ()	0.307 ()	0.083	0.000 ()	0.417 ()	1.300 ()
Mascardi (nc) (Argentina) [65-67]	-0.023	-1.400 ()	0.045 (*)	0.151	1.555 ()	0.040 (*)	0.937 ()
Quetihue (c) (Argentina) [65-67]	-0.051	0.900 ()	0.144 ()	0.104	-1.428 ()	0.081 ()	-0.806 ()
Quetihue (nc) (Argentina) [65-67]	-0.043	1.636 ()	0.073 ()	0.079	-1.750 ()	0.053 ()	-0.627 ()
Safariland (Argentina) [65-67]	-0.035	0.031 ()	0.432 ()	0.097	-0.142 ()	0.406 ()	-0.182 ()
Plant - Hervibore (4)							

Arid grasslands in Marathon (USA) [68]	-0.168	4.571 (*)	0.000 (*)	1.193	-1.256 ()	0.112 ()	2.696 ()
Arid grasslands in Altuda (USA) [68]	-0.215	3.200 (*)	0.001 (*)	1.316	-1.489 ()	0.048 (*)	1.226 ()
Whole country (Britain) [69]	-0.016	-0.500 ()	0.198 ()	1.100	0.875 ()	0.177 ()	0.693 ()
Whole country (Finland) [69]	-0.055	0.651 ()	0.275 ()	1.420	0.000 ()	0.240 ()	-0.320 ()
Plant - Seed Disperser (5)							
Forest (Papa New Guinea) [70]	-0.030	0.075 ()	0.427 ()	1.131	-0.588 ()	0.246 ()	-0.537 ()
Semideciduous tropical forest (Panama) [71]	-0.689	0.276 ()	0.322 ()	1.081	-0.14 ()	0.449 ()	-0.950 ()
Neotropical forest (Trinidad) [72]	-0.026	0.858 ()	0.192 ()	1.077	-0.736 ()	0.231 ()	-0.178 ()
Birds and Berries. Calton (England) [72]	-0.087	0.500 ()	0.346 ()	0.796	0.333 ()	0.358 ()	0.965 ()
Temperate woodland (Britain) [73]	-0.459	0.814 ()	0.266 ()	0.926	-0.561 ()	0.470 ()	1.559 ()
Anemone-Fish (1)							
Coral reefs [74]	-0.064	0.063 ()	0.483 ()	1.085	-0.633 ()	0.322 ()	-1.025 ()

Table 2. Empirical bimodal networks from different backgrounds appearing in Fig.4 and their values of Pearson’s correlation nestedness η . The z-score and P-values are calculated with respect to the random null model, and the “z-score with correlations” with the null model restricted to the actual correlation coefficient r of the network. As above, the asterisks * stand for z-values larger than 3 (in absolute value) and P-values smaller than the threshold 0.05.

FIGURE CAPTIONS

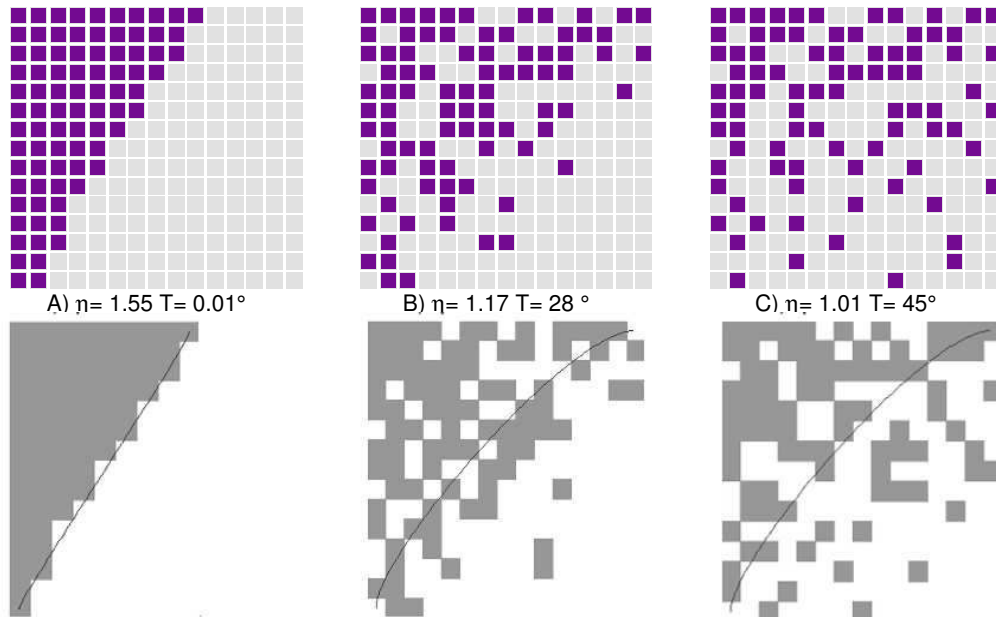


Figure 1. The figure shows three different connectivity matrices with different levels of nestedness as measured by (i) our new nestedness index [Eq.(6)] and (ii) the standard nestedness “temperature’ calculator”. As can be readily seen, the most packed matrix corresponds to a very low temperature and to a high nestedness index ($\eta > 1$) and, reciprocally, the least packed one exhibits a high temperature and an index close to its expected value for a random network ($\eta \simeq 1$).

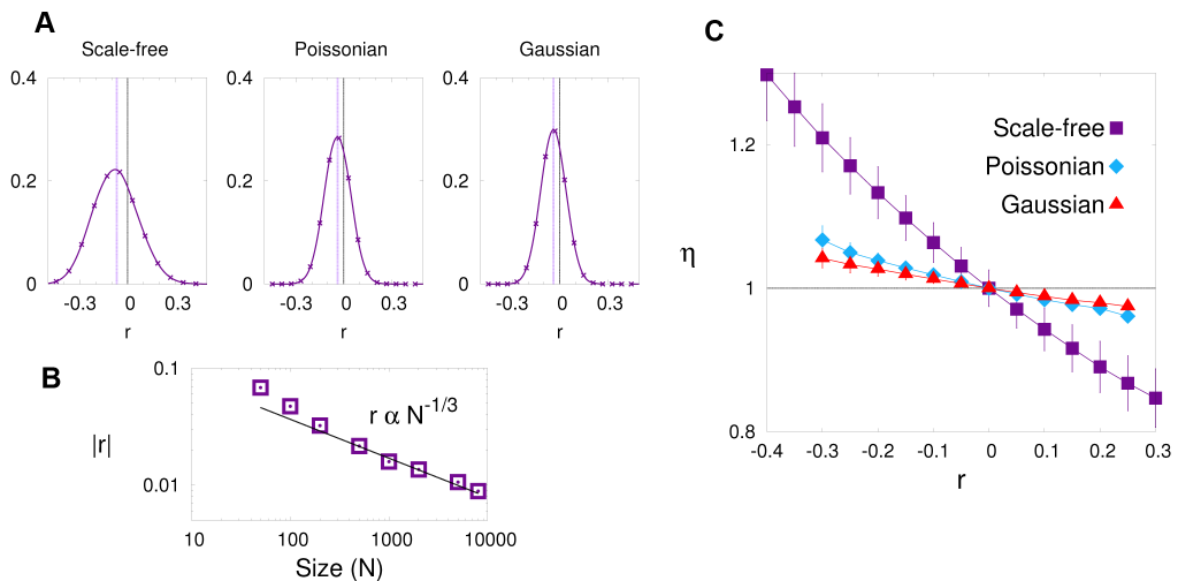


Figure 2. A: Correlation coefficient, r , and nestedness η for 10^6 networks generated independently using the configuration model with $N = 50$ nodes and $\langle k \rangle = 5$ and (from left to right) scale-free (with exponent $\gamma = 2.25$), Poissonian, and Gaussian ($\sigma^2 = 10$) degree distributions. B: Pearson's correlation coefficient as a function of network size for scale free networks with $\gamma = 2.25$. C: averaged nestedness (with error bars corresponding to one standard deviation) as a function of Pearson's correlation index r in random (scale-free, Poissonian, and Gaussian) networks (as in the left panel). These curves are obtained employing the Wang-Landau algorithm as described in Appendix C. All three curves show a positive (almost linear) correlation between disassortativity and nestedness: more disassortative networks are more nested. By restricting the corresponding configuration ensembles to their corresponding subsets in which r is kept fixed it is possible to define a more constraint null model as discussed in section.

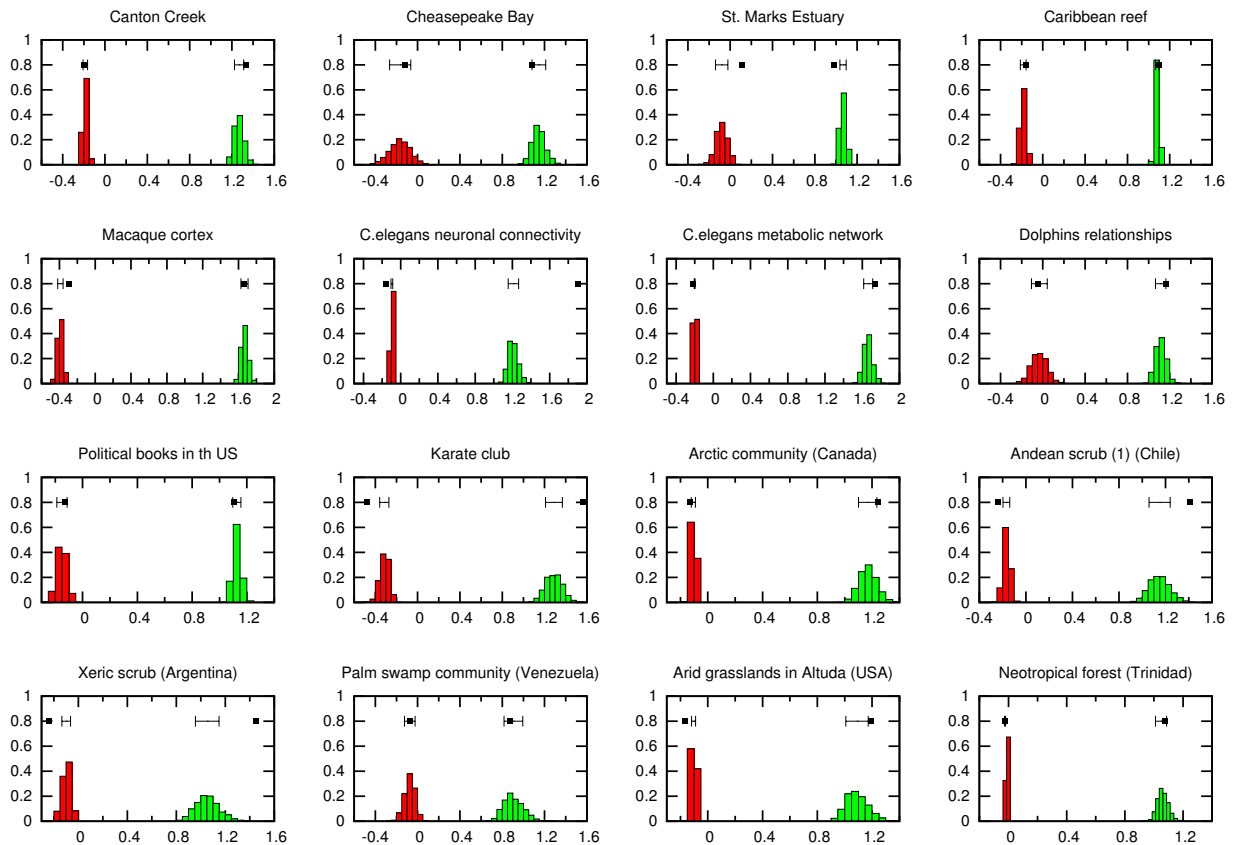


Figure 3. Probability distribution of Pearson's coefficient r and of the nestedness coefficient, η , as measured in degree-preserving randomizations of a subset of 16 (out of a total of 60) real empirical networks (as described and referenced in Table 1 and 2). The actual empirical values in the real network are marked with a black box and compared (also in black) with a segment centered at the mean value of the random ensemble (configuration model) with width equal to one standard deviation. In most cases but not all, the empirical values lie in or near the corresponding interval, suggesting that typically empirical networks are not significantly more assortative/nested than randomly expected.

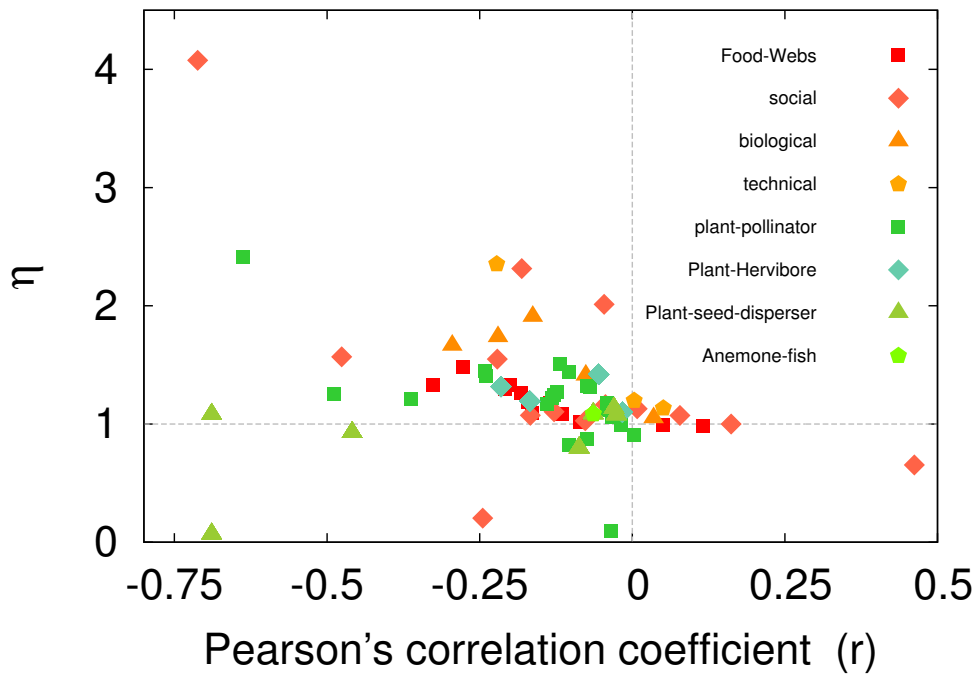


Figure 4. Nestedness against assortativity (as measured by Pearson's correlation coefficient) for data on a variety of networks. Warm-coloured items correspond to unimodal networks (see Table 1), and green ones to bipartite networks of different kinds (see Table 2).

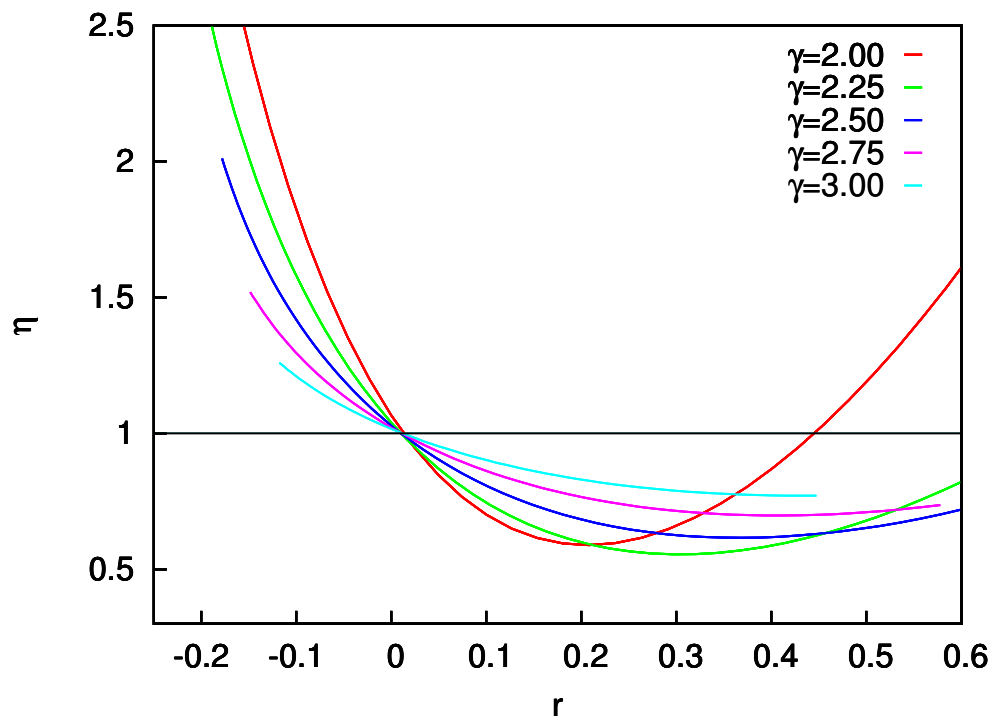


Figure A1. Nestedness against assortativity (as measured by Pearson's correlation coefficient, r) for scale-free networks with different values of the degree-distribution exponent, γ . $\langle k \rangle = 10$, $N = 1000$.

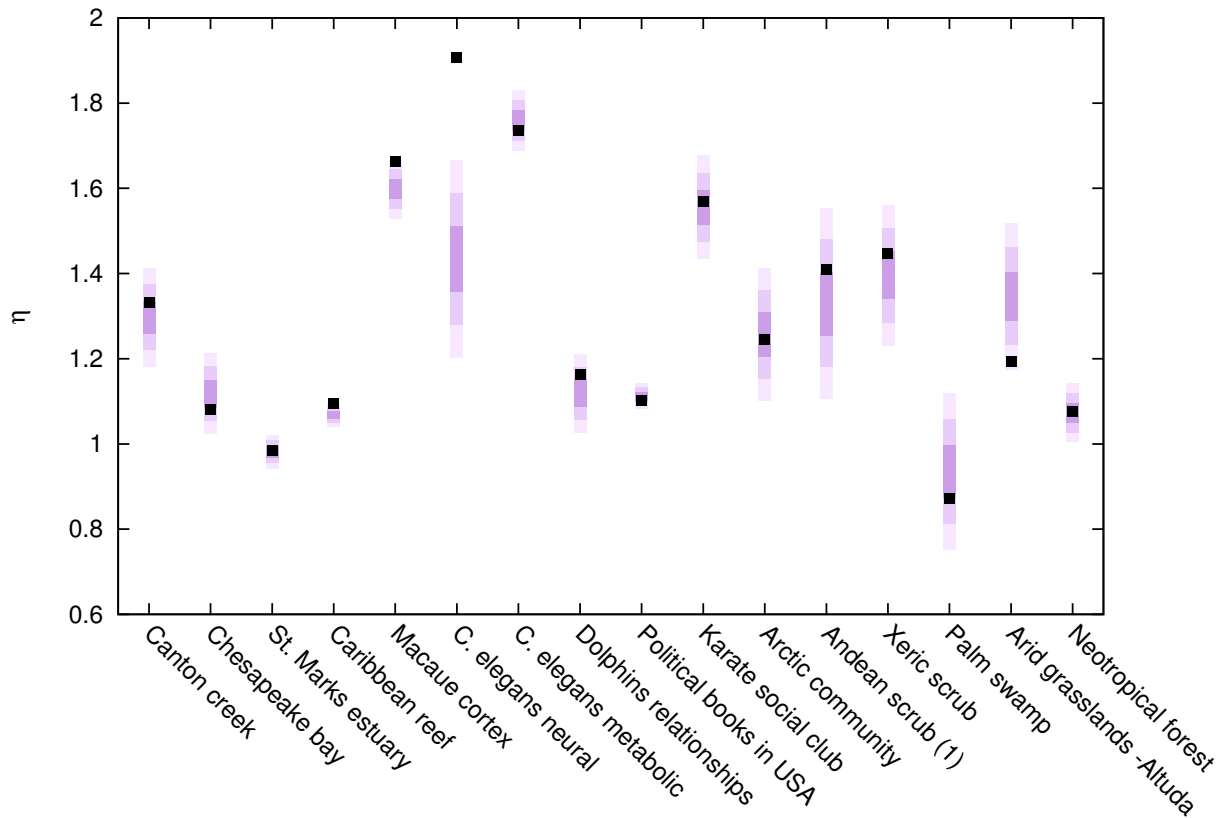


Figure A2. Averaged nestedness index, η , as measured in the second null model in which the value of r is preserved. The actual value of η in the real network is marked with a black square, while the coloured intervals corresponds to one, two and three standard deviations respectively. In most cases the empirical value lies in or near the corresponding interval. Allowing for two or three standard deviations essentially all empirical points yield within the corresponding interval.